

# ACOUSTOOPTIC BRAGG DIFFRACTION IN A SPHERICAL WAVEGUIDE – THEORY AND RECENT EXPERIMENT\*

W. Chen<sup>1)</sup>, P. Le<sup>1)</sup>, S. C. Tsai<sup>2)</sup>, and C. S. Tsai<sup>1,3)</sup>

<sup>1)</sup> Dept. of Electrical and Computer Engineering, Univ. of California, Irvine, CA, USA

<sup>2)</sup> Dept. of Chemical Engineering, California State Univ., Long Beach, CA, USA

<sup>3)</sup> Inst. for Applied Science and Engineering Research, Academia Sinica, Nankang, Taipei, Taiwan 11529

Correspondence: C. S. Tsai, Phone: (886) 2-2782-6670; Fax: (886) 2-2782-6672; E-mail: cstsai@phys.sinica.edu.tw

## 1. Introduction

We previously proposed a spherical substrate<sup>[1]</sup> that can simultaneously guide, collimate, and focus the light beams, and thus serves as an alternate to planar substrate for realization of acoustooptic (AO) Bragg cell modulators and related devices. Some encouraging experimental results on AO Bragg diffraction at relatively low surface acoustic wave (SAW) center frequency, namely, 245 MHz using a LiNbO<sub>3</sub> hemispherical block were reported<sup>[1]</sup>. In this paper we report a theoretical treatment for such spherical guided-wave AO interactions together with new experimental results at significantly higher SAW center frequency and bandwidth, namely, 500 and 250 MHz, respectively.

A focused light beam entering at point P on the rim of the base plane of a hemisphere block is guided, collimated at the top of the hemisphere, and refocused at point P' on the opposite side of the rim (see Fig. 1). Now, if an interdigital transducer of proper orientation and center frequency is deposited on the top of the hemisphere (see Fig. 2), the SAW generated will interact with the incident guided-light wave in a manner similar to the AO interaction in the planar waveguides<sup>[2]</sup>. In the case of Bragg diffraction, the diffracted light propagates at twice the Bragg angle from the incident light, and focuses at a point D on the rim of the base plane. As the frequency of the SAW is varied, the focal spot of the Bragg diffracted light is scanned along the rim.

## 2. Theoretical Treatment

A summary of the theoretical treatment and the experimental results are presented as follows.

### 2.1 Asymptotic Guided-Light Waves in An Anisotropic and Homogeneous Spherical Surface

Assuming that a layer with a refractive index greater than that of an anisotropic and homogeneous hemisphere substrate is formed on its spherical surface. For the case in which the thickness of the layer is much smaller than the radius ( $a$ ) of the hemisphere, excitation and propagation of well-confined guided optical waves can be readily facilitated. In addition, for simplicity two-dimensional approximation together with the asymptotic approximations are imposed. Thus, the following two-dimensional Laplacian in spherical coordinates (with unit vectors  $\hat{r}$ ,  $\hat{\theta}$ , and  $\hat{\phi}$ )<sup>[3]</sup> with the radius " $a$ " can be conveniently adopted.

From the Maxwells' equations in terms of the electric field quantities  $\vec{E}$  and  $\vec{D}$ , and the magnetic field quantities  $\vec{H}$  and  $\vec{B}$  at a harmonic time dependence  $\exp^{i\omega t}$ , the wave equation for the electric field of the light wave is determined. We assume that  $\vec{E}$  takes an asymptotic expansion (with the wave number  $k_0 \rightarrow \infty$ ) of the following form:

$$\vec{E} \sim e^{ik_0\psi} \sum_{n=0}^{\infty} \frac{\vec{E}_n}{(ik_0)^n} \quad (2.1)$$

where the phase function  $\psi$  and the expansion coefficients  $\vec{E}_n$  are functions of the coordinates only,

\* This work was supported by Academia Sinica, Taiwan and UC MICRO Project, U.S.A.

and the wave number in free-space  $k_0 = (\omega/c)$ . After inserting Eq. (2.1) into the wave equation for  $\bar{E}$  and keeping only the first term  $\bar{E}_0$ , the asymptotic solutions for  $\bar{E}_0$  are obtained as follows:

$$\bar{E}^{(0)} \sim \left( e^{ik_0 \sqrt{\varepsilon_1} a \theta} \right) (\sin \theta)^{-1/2} \hat{\gamma} \quad (\text{Ordinary or TM-Wave}) \quad (2.2a)$$

and

$$\bar{E}^{(e)} \sim \left( e^{ik_0 \sqrt{\varepsilon_2} a \theta} \right) (\sin \theta)^{-1/2} \hat{\phi} \quad (\text{Extraordinary or TE-Wave}) \quad (2.2b)$$

where  $\varepsilon_1$  and  $\varepsilon_2$  are the two principal dielectric constants of a uniaxial crystal such as LiNbO<sub>3</sub>. Thus, we have shown that under the situation with weak anisotropy and paraxial approximation, there exist two independently polarized waves, namely, the ordinary and the extraordinary waves which polarize, respectively, along  $\hat{r}$  and  $\hat{\phi}$  direction, i.e., the TM- and TE-waves (see Fig. 3).

## 2.2. Asymptotic Rayleigh SAW In An Isotropic And Homogeneous Spherical Surface

Referring to Fig. 3 again and following the same procedure as that in Section 2.1, the following asymptotic solutions for the components of the acoustic strain field are obtained:

$$S_2 \equiv S_{\theta\theta} \sim \left( e^{ika\theta} \right) (\sin \theta)^{-1/2} \quad (2.3a)$$

$$S_6 \equiv S_{r\theta} \sim \left( e^{ika\theta} \right) (\sin \theta)^{-1/2} \quad (2.3b)$$

where  $K \equiv \Omega/V_R$ ,  $\Omega$  and  $V_R$  designate the acoustic radian frequency and the Rayleigh wave velocity, respectively. It is to be noted that the solutions for the SAW take the same simple form as the light waves.

## 2.3 Approximate Solution for Bragg-Diffracted Light Wave

In order to calculate the AO Bragg diffraction we first express both the guided-optical waves and the SAW in terms of the same coordinate system as depicted in Fig. 2. Thus, the new coordinate system ( $X'$ ,  $Y'$ ,  $Z'$ -axes) shown in Fig. 2 is generated by rotating the old one ( $X$ -,  $Y$ -,  $Z$ -axes) by an angle  $(\pi/2 + \gamma)$  with respect to the  $Y$ -axis. For any given angle  $\gamma$  the intersection point between the light rays and the acoustic rays can be determined. For example, for an incident light of the TE-modes, i.e., the guided-modes that are polarized along the  $\theta$ -axis, the point source for the diffracted light waves at the intersection point is readily obtained. Thus, the total diffracted light wave resulting from the distribution of point sources is determined as follows:

$$U_d(\theta, \phi) = \int_{-\alpha}^{\alpha} d\phi \int_{-\beta}^{\beta} d\phi' (\omega_d/c)^2 a^2 k_d n^4 P_{12} S_2(\theta, \phi) U_i(\theta', \phi') \frac{e^{ik_d a \theta''}}{\sqrt{\sin \theta''}} \quad (2.4)$$

where the wave number of the diffracted light wave  $k_d$  is given by  $n(\omega \pm \Omega)/c$ , in which  $n$  = effective index of refraction,  $\omega$  = angular frequency of the incident light,  $\Omega$  = angular frequency of the SAW, and  $P_{12}$  is the relevant photoelastic coefficient that couples the strain field  $S_2(\theta, \phi)$  with the incident optical wave  $U_i(\theta', \phi')$ , and the double primed coordinate  $\theta''$  is related to the unprimed coordinate through a definite coordinate transformation. Note that for given  $\phi$  and  $\phi'$ ,  $\theta$ ,  $\theta'$ , and  $\theta''$  can be determined in terms of  $\phi$  and  $\phi'$ .

For the case with small divergence angles for both acoustic and optical waves, namely,  $|\phi'| < 1, |\phi| < 1$ , and under the Bragg condition we obtain the expression for the Bragg-diffraction efficiency  $\eta_{dBragg}$  as follows:

$$\eta_{dBragg} \equiv |U_d|^2 / A^2 = \left| (\omega_d/c)^2 k_d n^4 P_{12} 4B a^2 \alpha \beta \right|^2 \quad (2.5)$$

where A and B are the two constants to be determined by Poynting's vectors of the SAW and the incident optical wave. Note that the Bragg diffraction efficiency under perfect phase matching condition is a linear function of acoustic power as  $|\eta_B|^2$  is proportional to the acoustic power, and increases quadratically with the angular spread ( $\beta$ ) of the incident light beam.

### 3. Experimental Results

In the experimental study, the guiding layers on the LiNbO<sub>3</sub> hemispherical blocks (3.1 cm dia) were formed using the TI method, and a pair of tilted-finger chirp SAW transducers (finger aperture of 0.5 mm) of 500 MHz center frequency and 250 MHz bandwidth were fabricated using the lift-off technique. The Bragg diffraction measurements were performed at 0.6328  $\mu\text{m}$  optical wavelength using the same arrangement as in Ref. [1]. Measured results are now presented as follows.

The Bragg diffraction efficiency versus the RF frequency shows the two 3dB frequencies covering a frequency band from 345 to 590 MHz, i. e. a bandwidth of 245 MHz that agrees with the design value. The plot of Bragg diffraction efficiency versus the RF drive power at 530 MHz shows a diffraction efficiency of 28% at an RF drive power of 4.4 watt. Also, the linear dependence of the diffraction efficiency on the RF drive power shown in the plot was in agreement with the theoretical prediction.

Fig. 4 shows the intensity profiles of both the undiffracted light beam (a) and the Bragg-diffracted light beam (b) along the rim of the hemisphere base plane measured using a CCD photo detector array. The profile of the undiffracted light beam clearly shows a well focused spot with low sidelobe level and that of the Bragg-diffracted light beam shows similar beam quality.

The Bragg-diffracted light beam was scanned along the rim of the base plane by varying the acoustic frequency. From Fig. 4(c), we see that the diffracted light beams were resolved spatially (based on Rayleigh criterion) at a frequency differential of 4 MHz. In other words, the measured frequency resolution ( $\Delta f$ ) relevant to applications such as light beam scanners and RF spectrum analyzers was 4 MHz. Thus, under a 245 MHz bandwidth, the corresponding number of resolvable channels was approximately 60. Finally, the throughput efficiency measured between the input port and the output port varied from -9 to -11 dB.

### 4. Conclusions

The method of lowest-order asymptotic expansion has led to simple solutions for optical waves along a spherical surface of both isotropic and weak anisotropic substrates. Using the same method similar form of solutions are obtained for Rayleigh SAW. The AO interactions between such form of optical waves and SAW are analyzed using Green's function technique. Like the case with a planar waveguide, when the phase-matching condition is satisfied the interaction reduces to the well-known Bragg diffraction, and the diffracted light takes a relatively simple form in terms of all related physical parameters. Bragg diffraction experiments using a LiNbO<sub>3</sub> hemisphere block (3.1 cm Dia) at the optical wavelength of 0.6328  $\mu\text{m}$  and the center SAW frequency of 500 MHz involve the physical dimensions that satisfy the assumptions required in the theoretical treatment. High diffraction efficiency and large bandwidth as well as high-quality focused spots of both the undiffracted and the Bragg-diffracted light beams obtained suggest potential use of the spherical surface for realization of integrated AO device modules<sup>[2]</sup>.

### Reference

- [1] Q. Li, C. S. Tsai, S. Sottini, and C. C. Lee, *Appl. Phys. Lett.*, Vol. **46** (8), 707-710 (April 1985).
- [2] See, for example, the many references cited in C. S. Tsai, *Proc. IEEE*, Vol. **84**, 853-869 (1996).
- [3] S. Ramo, J. R. Whinnery, and T. Van Duzer, *Fields and Waves in Communication Electronics*, New York: Wiley (1984).

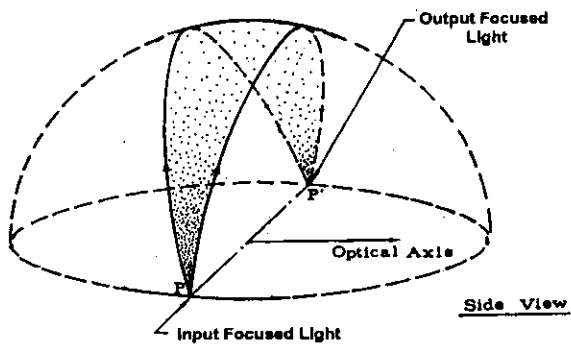


Fig. 1 A Hemispherical Waveguiding Surface

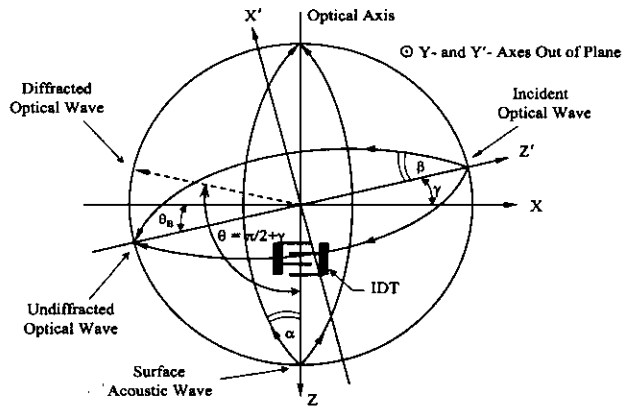


Fig. 2 Top View of A Hemispherical Surface for Acousto-optic Interaction

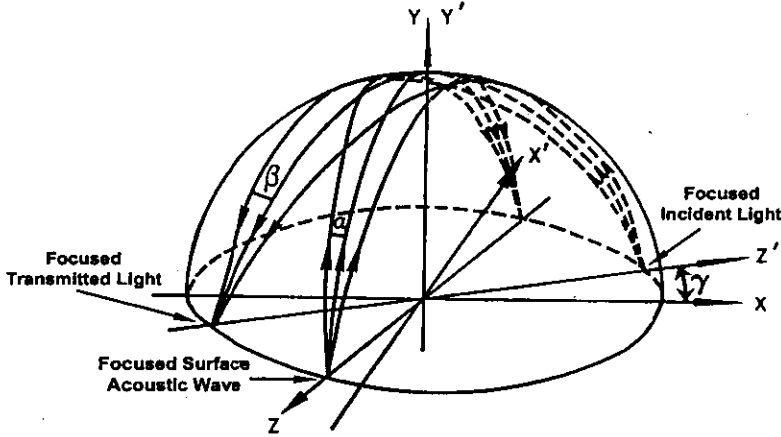
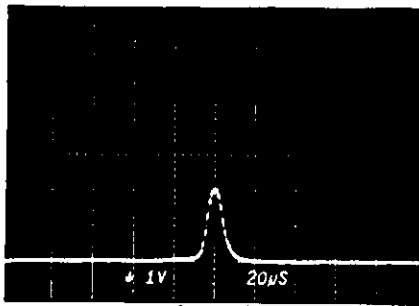
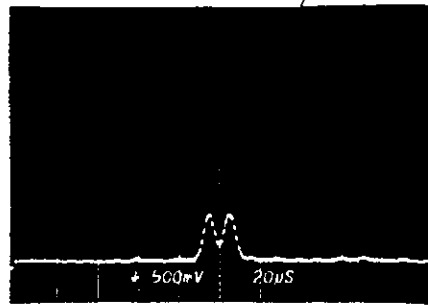


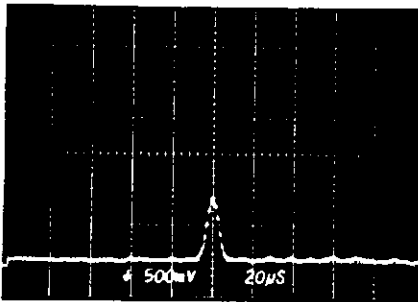
Fig. 3 Side View of A Hemisphere for Acousto-optic Interaction



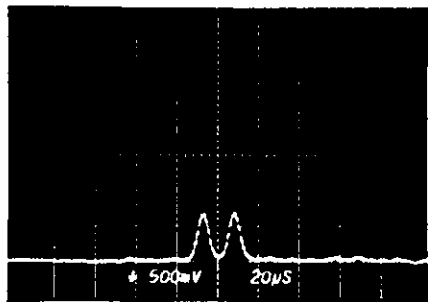
(a)



(c)



(b)



(d)

Fig. 4 Beam Profiles of AO Bragg Diffraction in Spherical Waveguide

(a). Undiffracted Light

(b). Single Diffracted Light (at  $f_a = 376$  MHz)

(c). Double Diffracted Light (at  $f_{a1} = 376$  MHz,  $f_{a2} = 372$  MHz)

(d). Double Diffracted Light (at  $f_{a1} = 376$  MHz,  $f_{a2} = 370$  MHz)

[Light Wavelength =  $0.63 \mu\text{m}$ , Horizontal scale =  $15.6 \mu\text{m}/\text{major div.}$ ]